OBSTETRICS

Assessing maternal cardiac function by obstetricians: technique and reference ranges

Check for updates

Greggory R. DeVore, MD; Bardo Polanco, PhD, RDMS

BACKGROUND: A strong body of evidence has now coalesced indicating that some obstetrical syndromes may result from maladaptive responses of the maternal cardiovascular system. Longitudinal studies have shown that these changes are complex and present before the clinical recognition of preeclampsia and fetal growth restriction, suggesting that hemodynamic maladaptation may play an etiologic role in obstetrical complications. Chronic hypertension is one of the most frequent complications of pregnancy, and recent evidence suggests that control of mild hypertension in early pregnancy improves outcome. The management of chronic hypertension can be improved by understanding specific cardiovascular hemodynamic abnormalities such as increased cardiac output or increased systemic vascular resistance, which can respond to either beta or calcium channel blockers, depending on the hemodynamic findings. Evaluation of maternal cardiac function has not been previously available to obstetrical healthcare providers using diagnostic ultrasound equipment used for fetal evaluation.

OBJECTIVE: Obstetrical ultrasound machines may be configured for various probes (endovaginal, abdominal, 3D/4D, and cardiac). This study used a cardiac probe placed in the suprasternal notch to image and measure the descending aorta diameter and the velocity time integral using pulsed and continuous wave Doppler ultrasound in normal pregnant women between 11 and 39 weeks of gestation. These measurements were followed by computation of maternal left ventricular preload, afterload, contractility, and blood flow.

STUDY DESIGN: This was a prospective cross-sectional study. A total of 400 pregnant women were recruited between 11 and 39 weeks of gestation. Imaging of the maternal aortic arch was performed by placing a cardiac probe in the suprasternal notch to identify the aortic arch using 2D and color Doppler ultrasound. The end-systolic diameter of the aorta was measured at the junction of the left subclavian artery with the descending aorta, which was followed by insonation of the descending aorta to obtain the Doppler waveform. Following insonation of the descending aorta, measurements of the aortic diameter, velocity time integral, ejection time, mean pressure gradient, heart rate, maternal weight and height, and systolic and diastolic blood pressures were entered into an Excel spreadsheet to compute the following: (1) preload measurements of stroke volume, stroke volume index, and stroke work index; (2) afterload measurements of systemic vascular resistance and the potential-to-kinetic energy ratio; (3) contractility measurements of inotropy and the Smith—Madigan inotropy index; and (4) blood flow measurements of cardiac output and the cardiac output index. Fractional polynomial regression analysis was performed for each of the above measurements using gestational age as the independent variable.

RESULTS: The diastolic and mean arterial blood pressure decreased from 11 to 18 weeks of gestation and then increased until term. The afterload measurements demonstrated similar characteristics, as all values decreased from 11 weeks until the mid and late second trimester, after which all values increased until term. Changes in contractility demonstrated an increase from 11 weeks to 25 to 28 weeks, followed by a decline until term. Changes in blood flow demonstrated an increase from 11 to 27 weeks and then declined until term. The continuous wave Doppler values were greater than the pulsed Doppler values except for the contractility measurements. Examples of abnormal cardiac measurements were identified in pregnant patients with hypertension and fetal growth restriction. An Excel calculator was created to provide quick computation of z-score measurements and their corresponding centiles described in this study.

CONCLUSION: The technique for evaluation of maternal cardiac function described in this study would allow screening of maternal left ventricular preload, afterload, contractility, and blood flow in the obstetrical clinical milieu once a cardiac probe is acquired for obstetrical ultrasound machines used for fetal evaluation. The above measurements would allow the clinician to select appropriate hypertensive medication on the basis of the results of the evaluation of the maternal left ventricle.

Key words: afterload, blood flow, cardiac output, cardiac output index, continuous wave Doppler, contractility, potential-to-kinetic energy ratio inotropy, preload, pulsed Doppler, Smith—Madigan inotropy index, stroke volume, stroke volume index, stroke work index, systemic vascular resistance

Introduction

Successful hemochorial placentation requires major adaptations in maternal hemodynamics, whereas the absence of such adaptations can result in preeclampsia and other maternal disorders.[1] The key features, occurring early in the first trimester, include an increase in cardiac output (CO) and stroke volume (SV), and decreased systemic vascular resistance.[2–5] A strong body of evidence has now coalesced indicating that some obstetrical syndromes may result from maladaptive responses of the maternal cardiovascular system.[2,6–23] Longitudinal studies have shown that these changes are complex and are present before the clinical recognition of preeclampsia and fetal growth restriction, suggesting that hemodynamic maladaptation may play an etiologic role in obstetrical complications.[8] Recent studies have suggested the importance of evaluating the maternal CO and systemic vascular resistance in patients at risk for preeclampsia, growth restriction, and other complications of pregnancy.[11–14,16,18,20,24–26] Chronic hypertension is one of the most frequent complications of pregnancy, and recent evidence suggests that control of mild

Cite this article as: DeVore GR, Polanco B. Assessing maternal cardiac function by obstetricians: technique and reference ranges. Am J Obstet Gynecol 2023;229:155.e1-18.

0002-9378

© 2023 The Author(s). Published by Elsevier Inc. This is an open access article under the CC BY-NC-ND license (http://creativecommons.org/licenses/by-nc-nd/4.0/).

https://doi.org/10.1016/j.ajog.2023.01.003

Click Supplemental Materials and Video under article title in Contents at ajog.org

AJOG at a Glance

Why was this study conducted?

Alterations of maternal cardiac function are observed with pregnancy complications such as chronic hypertension, preeclampsia, and fetal growth restriction. To enable obstetrical clinicians to evaluate maternal cardiac function, this study measured left ventricular function by imaging the descending aorta from the suprasternal notch to create reference intervals for measurements of preload, afterload, contractility, and blood flow.

Key findings

The results from the measurement of left ventricular function by imaging of the descending aorta are similar to those of previous studies that used imaging of the ascending aorta. The cardiac probe used in this study is available on all ultrasound machines used for fetal imaging. The ability to measure cardiac output from the descending aorta is a potential tool that could be used for screening pregnant women with chronic hypertension, preeclampsia, fetal growth restriction, and other diseases of pregnancy that may alter cardiac function. The reported methodology is feasible, easily accessible to every obstetrical sonographer, allows cardiac ultrasound measurements to be obtained under direct vision, and provides data similar to those reported using other technologies.

What does this add to what is known?

This study used the suprasternal notch imaging of the descending aorta to compute maternal left ventricular function in a normal population and provide reference interval tables, graphs, and a calculator to compute z-scores and their corresponding centiles using gestational age as the independent variable.

hypertension in early pregnancy improves outcome.[27,28] The management of chronic hypertension can be improved by understanding specific cardiovascular hemodynamic abnormalities such as increased CO or increased systemic vascular resistance, which can respond to either beta or calcium channel blockers, depending on the hemodynamic findings.[28]

Assessment of cardiovascular function has traditionally been the domain of cardiologists. However, the conceptual framework and techniques for assessment with ultrasound are straightforward and used by maternal–fetal medicine specialists to evaluate fetal cardiovascular status.[29–34] We envision that evaluation of the maternal cardiovascular system can become an integral part of obstetrical/maternal–fetal medicine practice. This can be accomplished by using conventional transducers available on ultrasound machines used in fetal imaging. Evaluation of maternal cardiac SV, CO, ejection fraction, and systemic vascular resistance has been reported using 17 invasive, partially invasive, and noninvasive methods to measure left ventricular function.[35] Of the noninvasive approaches, transthoracic echocardiography was the first ultrasound approach used in which ascending aortic blood flow was measured using a cardiac probe placed on the chest, wherein the apical 5-chamber and parasternal views are obtained with the patient lying in the left lateral position (Figure 1).[5,19,35–38] However, for pregnant women, the above cardiac images may be difficult to obtain, especially in the third trimester, when a large uterus compresses the diaphragm, resulting in decreased 2-dimensional echogenicity owing to cardiac axis displacement and engorgement of breast tissues.[3] Therefore, routine evaluation of maternal cardiac function using transthoracic echocardiography may not be practical using the above approach.

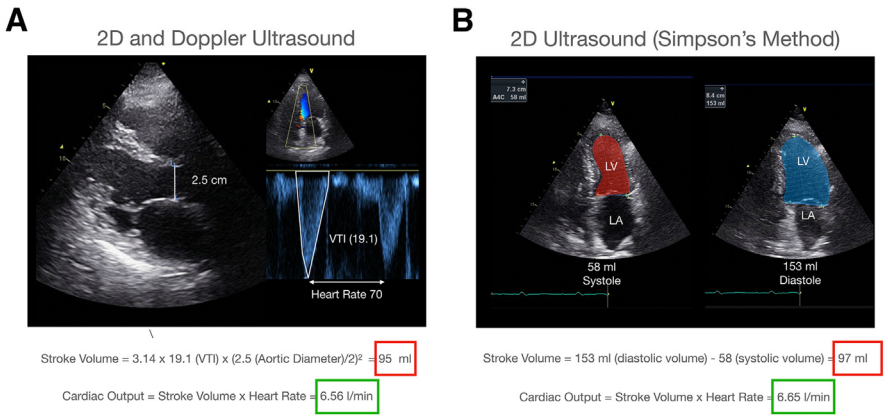
A second approach recently reported in pregnant women uses a continuous wave (CW) Doppler ultrasound probe, wherein the ultrasound beam is directed toward the ascending aorta using the suprasternal notch as the imaging window.[4,19,20,35,36,39–42] However, this method requires a dedicated ultrasound machine that only measures cardiac function and has no 2-dimensional or pulsed Doppler imaging options.[39,40] Another limitation is that the diameter of the aorta, used in the equation to compute the SV, is not measured but inferred from an algorithm using maternal height.[39]

Because ultrasound machines used for fetal evaluation are multifunctional, with the potential of using various probes (vaginal probe, abdominal probe, 3D and 4D probe, and cardiac probe), this study was designed to use a small footprint cardiac probe placed in the suprasternal notch (Figure 2), in which the 2-dimensional image of the ascending and descending aorta could be imaged and measured, followed by pulsed wave (PW) and CW Doppler interrogation of aortic blood flow, wherein the velocity time integral (VTI) was measured in normal pregnant women between 11 and 39 weeks of gestation, followed by computations of maternal left ventricular cardiac function (Figure 2). The clinical benefit of this study is that it could provide a practical approach for the obstetrical and maternal–fetal medicine specialist to obtain measurements that could be used to compute maternal cardiac function indices applicable for clinical management of hypertension, fetal growth restriction, and other pregnancy complications.[19]

Methods

This was a prospective cross-sectional study approved by Pearl IRB (Protocol 22-FEDC-102), Indianapolis, Indiana. Normal pregnant women were recruited between 11 and 39 weeks of pregnancy and agreed to participate in the study. Exclusion criteria included maternal hypertension (>140/90 mm Hg), diabetes mellitus, fetal abnormalities detected with diagnostic ultrasound, decreased fetal size (estimated fetal weight or abdominal circumference <10th centile), and multiple gestations.[43] Each patient underwent only 1 maternal ultrasound examination. The systolic and diastolic blood pressures

FIGURE 1
Echocardiographic measurements of maternal cardiac output



A, Two measurements required to compute cardiac output, aortic diameter imaged from the left parasternal view of the heart, and the pulsed Doppler of aortic blood flow waveform imaged from the apical view of the left ventricle. **B,** Imaging of the left ventricle at end-systole and end-diastole from which the volumes are computed using the Simpson method.

LA, left atrium; *LV*, left ventricle; *VTI*, velocity time integral.

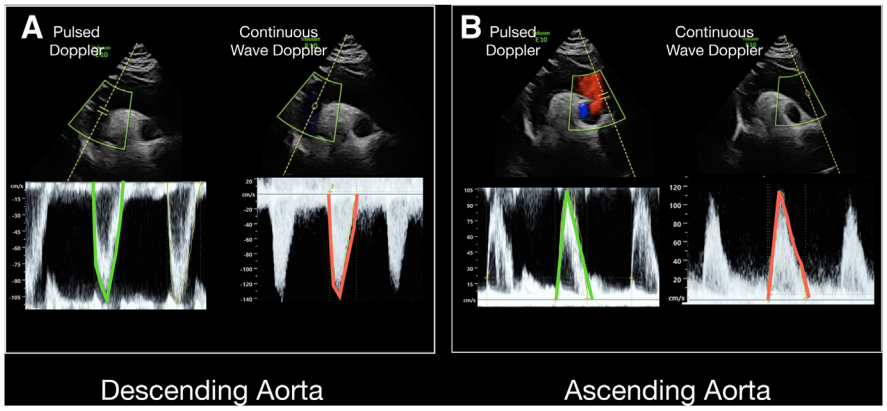
DeVore. Measurements of maternal cardiac function. Am J Obstet Gynecol 2023.

were obtained with an automated device and the maternal weight (pounds) and height (inches) that were converted to kilograms and centimeters, respectively (Table 1). First-, second-, and third-trimester fetal ultrasound evaluations of the fetus were performed using the General Electric Voluson Expert 21 and 22 (GE Healthcare Austria GmbH & Co OG, Zipf, Austria) following the guidelines recommended by the American Institute of Ultrasound in Medicine and the International Society of Ultrasound in Obstetrics and Gynecology.[45–47]

Imaging of the maternal aortic arch was performed by placing the cardiac probe in the suprasternal notch after placing a pillow under the shoulders to extend the head to the left with the patient in the supine position. Supplement 1 includes a video showing the placement of the ultrasound probe in the suprasternal notch, acquiring the Doppler waveforms, and measuring the Doppler waveforms. Two probes were used that were compatible with the GE Voluson Expert 21 and 22: M5Sc (footprint of 27.5×18.1 mm, 1–5 MHz) and 3SP (footprint of 23.4×20.2 mm, 1–5 MHz). This allowed for rotation and angulation of the ultrasound probe to image the aortic arch using 2D and color Doppler ultrasound (Supplement 1) (Figure 3). The end-systolic diameter of the aorta was measured at the junction of the left subclavian artery with the descending aorta and proximal to the innominate artery for the ascending aorta (Supplement 1) (Figure 3). Three to 4 Doppler waveforms were displayed on the screen in which Doppler peak velocities appeared to be similar (Supplement 1) (Figure 3).

Following the ultrasound examination, the measurements of maternal weight (pounds), height (inches), diastolic and systolic blood pressure, aortic VTI, ejection time, mean pressure gradient, heart rate, and aortic diameter (Figure 3) were entered into an Excel spreadsheet to compute the measurements listed in Tables 1 and 2 and Supplement 2.

FIGURE 2
Measurement of aortic blood flow from the descending and ascending aorta



A, Placement of the pulsed Doppler sample volume and the continuous wave Doppler in the descending aorta. **B,** Placement of the pulsed and continuous wave Doppler in the ascending aorta. The velocity time integral is indicated by the *green* and *orange* outline.

DeVore. Measurements of maternal cardiac function. Am J Obstet Gynecol 2023.

Statistical analysis

The measurements listed in Tables 1 and 2 and Supplement 2 were regressed against gestational age using 44 fractional polynomial regression equations to compute the reference intervals from which equations for the mean and standard deviation (SD) were derived (NCSS 2022; NCSS, LLC, Kaysville, UT).[48] The fractional polynomial regression equation with the highest R^2 was selected from the 44 equations. In addition to analysis using fractional polynomial equations, a *t* test was used to compare the mean values derived from the PW and CW Doppler measurements listed in Tables 1 and 2. The Lin concordance correlation coefficient was calculated between the average of 3 sequential VTI measurements and 1 VTI measurement to determine if there was a

TABLE 1
Measurements obtained at the time of the maternal ultrasound examination from the suprasternal notch

Demographics and measurements	Definition	Formula
Clinical data		
Age	Maternal age in y	
Maternal weight	Pounds	
Maternal weight	Kilograms	Weight (pounds)×0.453592
Maternal height	Inches	
Maternal height	Centimeters	Height (inches)×2.54
Body surface area[2]	The total surface area of the body (meters[2])	$\text{Square Root}\frac{\text{Weight (kg)} \times \text{Height (cm)}}{3600}$
Systolic blood pressure (mm Hg)	Maximum arterial pressure during contraction of the left ventricle of the heart	
Diastolic blood pressure (mm Hg)	Phase of the heartbeat when the heart muscle relaxes and allows the chambers to fill with blood	
Mean arterial pressure (mm Hg)	Average arterial pressure throughout 1 cardiac cycle, systole, and diastole	$\frac{\text{Systolic BP} + 2 \times \text{Diastolic BP}}{3}$
Ultrasound measurements from the suprasternal notch		
Aortic diameter (cm) (Figures 3 and 4)	Measured at the junction of the left subclavian artery and descending aorta	
Pulsed and continuous wave Doppler (Figure 2)		
Aortic velocity time integral (cm) (Figure 3)	The area within the spectral curve; indicates how far blood travels during systole	
Heart rate/min (Figure 3)		
Aortic ejection time (Figure 3)	The time interval from aortic valve opening to aortic valve closure	
Aortic mean pressure gradient (Figure 3)	Average arterial pressure throughout 1 cardiac cycle, systole, and diastole	

DeVore. Measurements of maternal cardiac function. Am J Obstet Gynecol 2023.

significant difference between 1 and 3 measurements. The same coefficient was used to evaluate intraobserver and interobserver measurements for the VTI and aortic diameter.

Comparison of stroke volume and cardiac output with the ultrasound cardiac output monitor

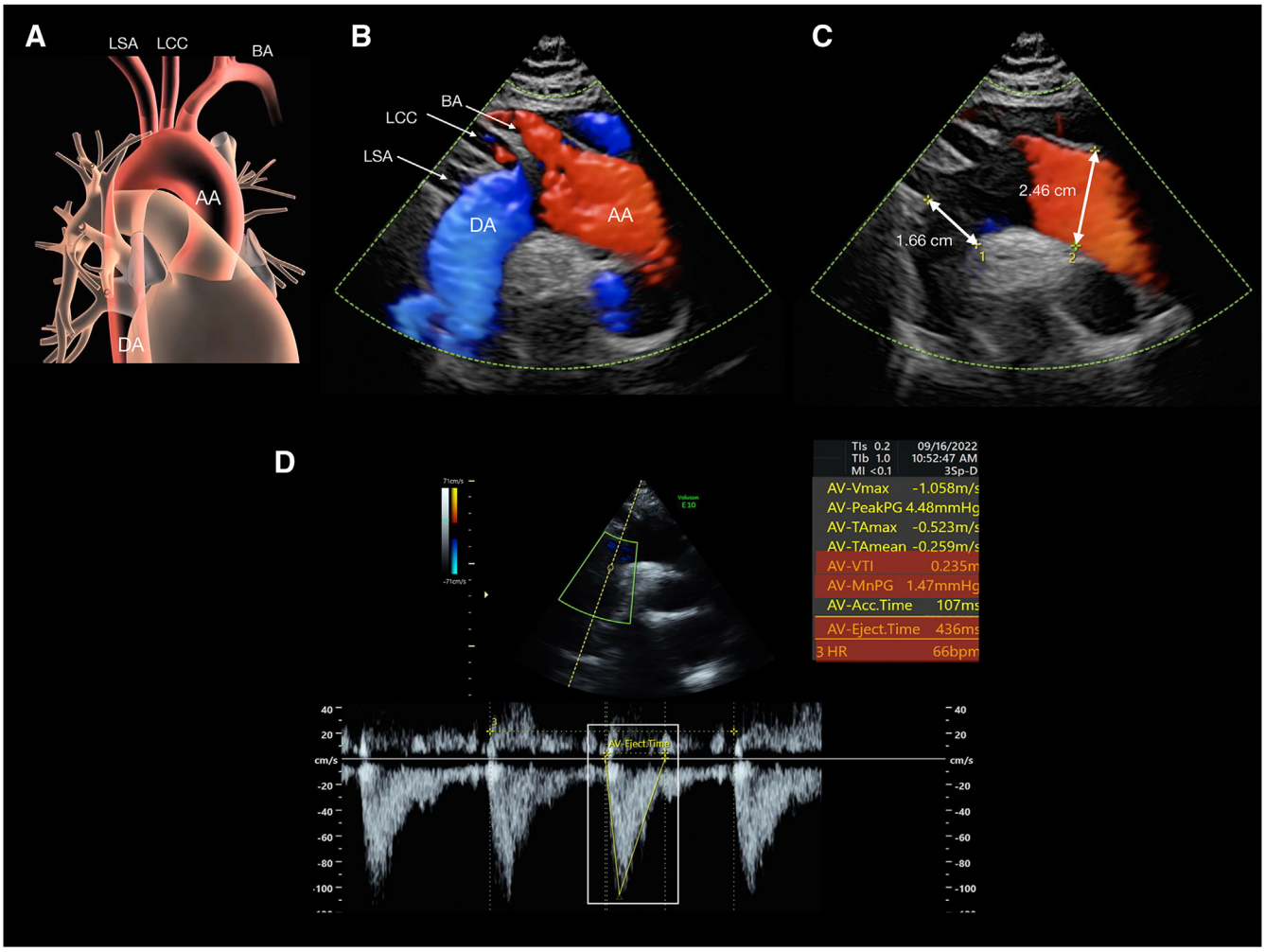
Vinayagam[40] reported results for SV and CO using the ultrasound cardiac output monitor (USCOM) device in which the aortic diameter at the level of the aortic valve was derived from the height of the patient (aortic annulus (cm)=0.010×height (cm)+0.25).[49] These measurements require the VTI and aortic diameter to compute the SV and the heart rate to compute the CO. Using the derived aortic diameter computed from the maternal height, we computed SV and CO from the CW VTI measured in the descending aorta, and then created the mean, 5th, and 95th reference centile graph to compare with the graphs from Figure 1 of the Vinayagam study.[50]

Results

Maternal demographics

A total of 400 patients who met the inclusion criteria were evaluated. Successful PW and CW Doppler measurements were obtained in 98% of patients for the descending aorta. Failed attempts at imaging the descending aorta were because of the inability to place the probe in the suprasternal notch because the latter was narrower than the probe head. However, the ascending aorta could only be imaged in 23 (5.7%) patients. Therefore, analysis of the ascending aorta Doppler measurements was not performed because of the small sample size. The ethnicities were 36% (N=143) Hispanic, 49% (N=196) White, 8% (N=31) Asian, and 8% (N=30) Black. The mean and SD values

FIGURE 3
Measurement of the ascending and descending aorta and the velocity time integral



A, Diagram of the aortic arch. **B,** Grayscale and color Doppler of the aortic arch vessels. **C,** Measurement of the ascending aorta (2.46 cm) and the descending aorta (1.66 cm) at the junction of the left subclavian artery and the descending aorta. **D,** Descending aorta measurements of the velocity time integral (AV-VTI), mean pressure gradient (AV-MnPG), ejection time (AV-Eject Time), and heart rate (3HR). These are the measurements required for computation of preload, afterload, contraction, and blood flow defined in Tables 2 and 3 and Supplement 1.

AA, ascending aorta; *AA*, aortic arch; *BA*, brachiocephalic artery; *DA*, descending aorta; *Eject.*, ejection; *HR*, heart rate; *LCC*, left common carotid artery; *LSA*, left subclavian artery; *MnPG*, mean pressure gradient; *PeakPG*, peak pressure gradient; *TAmax*, time average maximal velocity; *TAmean*, time average mean velocity; *Vmax*, maximal velocity; *VTI*, velocity time integral.

DeVore. Measurements of maternal cardiac function. Am J Obstet Gynecol 2023.

for the maternal weight, height, and age are listed in Table 3, with 32% (N=128) between 35 and 45 years of age (Table 3). Figure 4 demonstrates the 5th and 95th centile reference intervals for maternal weight (kg) and height (cm).

Maternal body surface area and blood pressure

Table 3 lists the mean and SD for the body surface area, aortic diameter, systolic pressure, diastolic pressure, and mean arterial pressure. The 5th, 50th, and 95th reference intervals for the maternal weight, height, body surface area, systolic blood pressure, diastolic blood pressure, and mean arterial pressure are illustrated in Figure 4. As expected, the maternal weight and body surface area increased with gestational age, whereas height did not change (Figure 4). The systolic pressure decreased from 11 to 16 weeks of gestation, then increased until 39 weeks of gestation. The diastolic and mean arterial pressures decreased from 11 to 18 weeks of gestation, and then increased until 39 weeks of gestation (Figure 4).

Fetal age and growth

Gestational ages ranged between 11 and 39 weeks. The mean fetal abdominal

TABLE 2
Cardiovascular measurements derived from the measurements in Table 1

Measurements	Definition	Formula
PRELOAD	The amount of ventricular stretch at the end of diastole	
Stroke volume (mL)	The volume of blood pumped out of the left ventricle of the heart during each systolic cardiac contraction	3.14×velocity time integral×(aortic diameter/2)^2
Stroke volume index	The volume of blood pumped by the heart with each beat divided by the body surface area	$\frac{\text{Stroke volume}}{\text{Body surface area}}$
Stroke work index	The stroke volume divided by the mean arterial pressure	$\frac{\text{Stroke volume}}{\text{Mean arterial pressure}}$
AFTERLOAD	The pressure the myocardial muscle must overcome to push blood out of the heart during systole	
Systemic vascular resistance (dynes×s/cm^5)	An index of arteriolar compliance or constriction throughout the body	$\frac{80 \times \text{mean arterial pressure}}{\text{Cardiac output}}$
Potential-to-kinetic energy ratio	Measure of arterial impedance	Potential energy/kinetic energy
CONTRACTILITY		
Contractility (inotropy) (watts)[44]	The force of contraction of the heart muscle	Potential+kinetic energy
Smith–Madigan inotropy index (watts/m^2)[44]	Total inotropy divided by body surface area	Inotropy/body surface area
CIRCULATION		
Cardiac output (liters/min)	The amount of blood pumped by the heart per min	$\frac{\text{Stroke volume} \times \text{heart rate}}{1000}$
Cardiac output index	The amount of blood pumped by the heart per min divided by the body surface area	$\frac{\text{Cardiac output}}{\text{Body surface area}}$

DeVore. Measurements of maternal cardiac function. Am J Obstet Gynecol 2023.

circumference centile was 55% (SD, 21%). The mean estimated fetal weight centile was 56% (SD, 20%).

Comparing the average of 3 measurements of the velocity time integral and a single measurement

The first 100 studies were selected from the database for PW Doppler measurements of the VTI, with each sample containing between 3 and 4 VTI Doppler waveforms. The 3 to 4 VTI waveforms were similar in peak velocity by visual inspection. Using the Lin concordance correlation coefficient, the correlation was 0.96 with the mean for 1 VTI measurement of 22.57 (SD, 5.69) and the average of 3 measurements of 22.28 (SD, 5.51). Therefore, there was no significant difference between the use of 1 and of 3 measurements for the final analysis.

Interobserver variation for the velocity time integral and the aortic diameter

Twenty samples were extracted from the database of PW Doppler measurements of the VTI and the aortic diameter. Using the Lin concordance correlation coefficient, the value for the VTI was 0.91 with a mean of 23.68 cm (SD, 5.38) for author G.R.D. and 23.81 cm (SD, 5.31) for author B.P., and for the aortic diameter, the correlation coefficient was 0.95 with a mean of 2.07 (SD, 0.22) and 2.1 (SD, 0.24), respectively.

Intraobserver variation for the velocity time integral and the aortic diameter

Twenty samples were extracted from the database of PW Doppler measurements of the VTI and the aortic diameter. The VTI waveform next to the waveform from which the study measurement was obtained was measured. The aortic diameter was measured from the image with no measurement compared with the same image with the measurement. The measurements were separated by >30 days. Using the Lin concordance correlation coefficient, the value for the VTI was 0.98 with a mean original measurement of 22.0 cm (SD, 4.59) for author G.R.D., and 21.6 cm (SD, 4.1) for the subsequent measurement. For the aortic diameter, the correlation coefficient was 0.92 with a mean of 1.95 (SD, 0.22) and 1.96 (SD, 0.21), respectively.

Cardiovascular measurements—descending aortic diameter

Figure 5 demonstrates that the descending aortic diameter increased by 1 mm from 10 to 22 weeks, did not change from 23 to 33 weeks, and decreased by 1 mm from 34 to 39 weeks. However, as a function of maternal

TABLE 3
Mean and standard deviation values for maternal measurements

Maternal age, height, weight, body surface area	Mean (SD)
Age	31 (6)
Maternal weight (pounds)	164 (34)
Maternal weight (kg)	74 (15)
Maternal height (inches)	63 (3)
Maternal height (cm)	160 (8)
Body surface area (m^2)	1.81 (0.2)
Aortic arch measurement	
Diameter (cm)	1.97 (0.24)
Blood pressure	
Systolic (mm Hg)	117 (51)
Diastolic (mm Hg)	69 (8.4)
Mean arterial pressure (mm Hg)	85 (9)

SD, standard deviation.
DeVore. Measurements of maternal cardiac function. Am J Obstet Gynecol 2023.

height, it increased from 130 to 160 cm (5 ft 2 in), after which it did not change as the maternal height increased.

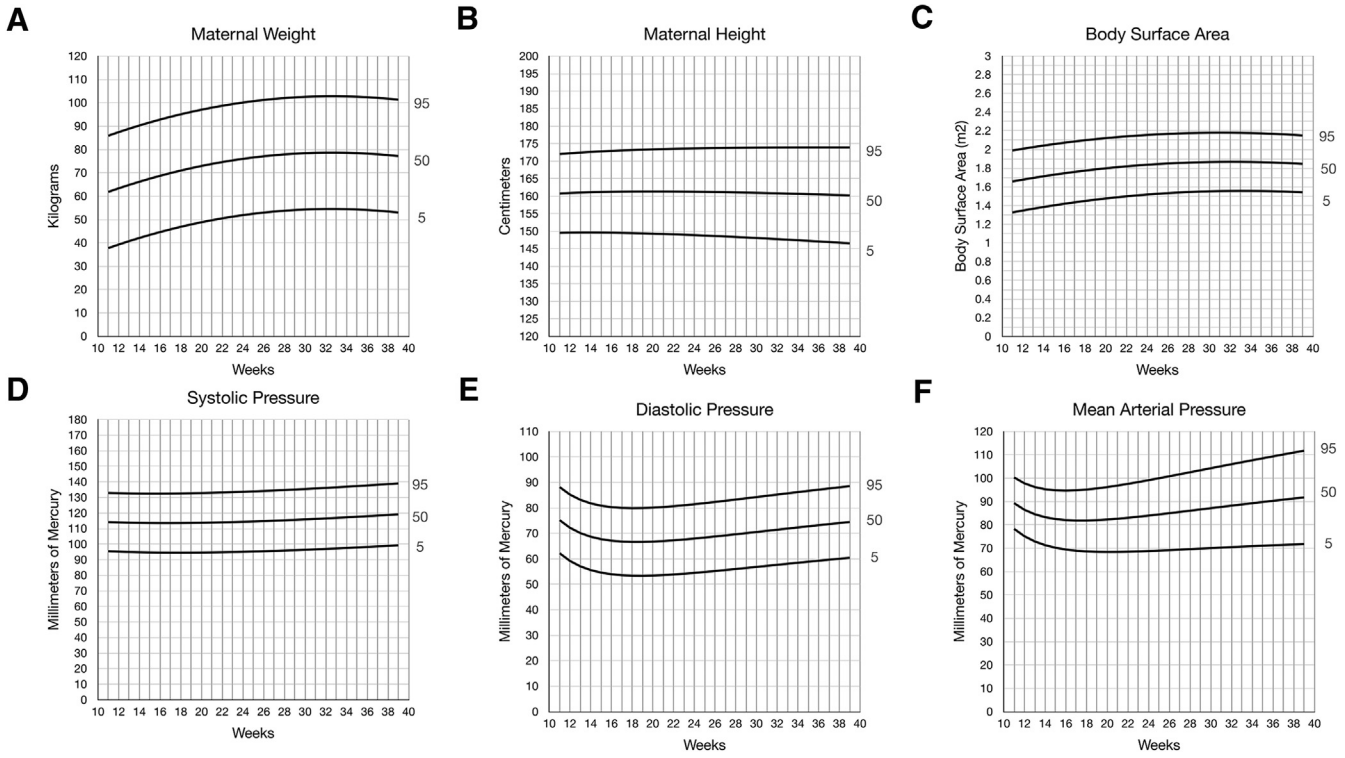
Cardiovascular measurements—heart rate and velocity time integral

The maternal heart rate increased from 70 to 90 beats per minute, with no difference between PW and CW measurements (Table 4; Figure 5). The VTI obtained with CW Doppler was significantly greater than when measured with PW Doppler (Table 4). Figure 5 demonstrates an initial increase in VTI from 11 to 18 weeks of gestation, followed by a decrease until 39 weeks.

Cardiovascular measurements—preload

The SV, SV index, and stroke work index increased from weeks 11 to 24, then

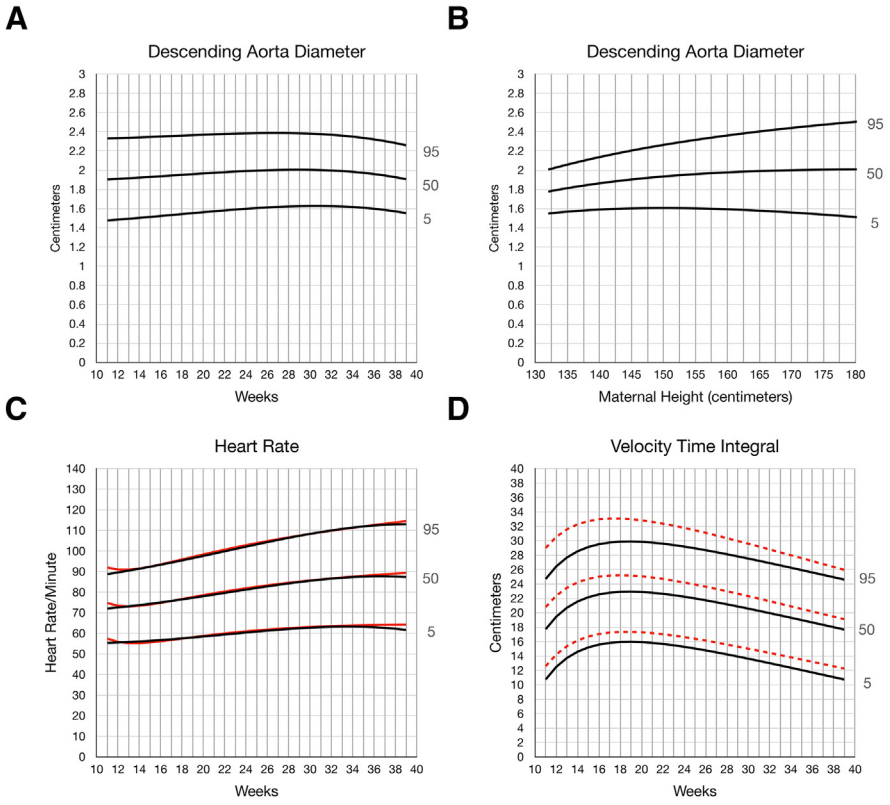
FIGURE 4
Maternal Non-Cardiac Measurements



Reference interval graphs of **A,** maternal weight **B,** height, **C,** body surface area, **D,** systolic pressure, **E,** diastolic pressure, and **F,** mean arterial pressure vs gestational age.

DeVore. Measurements of maternal cardiac function. Am J Obstet Gynecol 2023.

FIGURE 5
Maternal Cardiac Measurements



Reference interval graphs of the **A,** descending aorta diameter vs weeks of gestation, **B,** descending aorta diameter vs maternal height, **C,** heart rate, and **D,** velocity time integral.

DeVore. Measurements of maternal cardiac function. Am J Obstet Gynecol 2023.

decreased until term (Figure 6), with significantly higher values observed for the CW than the PW (Table 4).

Cardiovascular measurements—afterload

The systemic vascular resistance and the potential-to-kinetic energy ratio demonstrated similar characteristics as all values decreased from 11 weeks until 25 weeks for the systemic vascular resistance and 18 weeks for the potential-to-kinetic energy ratio, after which all values increased until term (Figure 7). The mean CW values for these 2 preload measurements were significantly lower than the mean PW values (Table 4).

Cardiovascular measurements—contractility

Figure 7 illustrates changes in inotropy and the Smith—Madigan inotropy index, wherein the values increased from 11 weeks, peeked at 28 weeks for inotropy and 25 weeks for the Smith—Madigan inotropy index, and then declined until term. The CW mean values were not different from the PW values (Table 4).

Cardiovascular measurements—blood flow

Figure 6 illustrates the changes in CO, and the CO index that increased from 11 to 27 weeks and then declined until term. The CW was significantly greater than the PW (Table 4).

Comment

Principal findings

Mean blood pressure is a function of the interaction between SV and systemic vascular resistance. For example, during pregnancy, as SV increases, systemic vascular resistance decreases to maintain homeostatic blood pressure. In 2014, Sanghavi and Rutherford[51] published a review of cardiovascular physiology in pregnancy, outlining the major changes that occur. Their findings are similar to the results of this study:

1. Peripheral vascular resistance decreases during the first trimester of pregnancy, with a nadir in the second trimester, and then increases until term (Figure 7).

2. SV increases early in pregnancy and reaches its nadir at the end of the second trimester, and then decreases until term (Figure 6).

3. CO increases from the first trimester until the second trimester and then decreases at term (Figure 6). The increased CO has been suggested to be the result of increased SV in the first 2 trimesters, but as the SV (Figure 6) decreases in the third trimester, the heart rate increases (Figure 5) from the second trimester until term.

4. The diastolic blood pressure and mean arterial pressure decrease from the first trimester to the mid-second trimester and then increase until term (Figure 4).

After reviewing the 17 different methodologies for measuring CO in pregnant women, the International Working Group on Maternal Hemodynamics stated the following: "Gestational age and, preferably, device-specific reference ranges for hemodynamic parameters in normal pregnancy constructed from data from women of differing ages and weights, would permit the interpretation of measured CO as a fraction of expected CO. Individual values can then be converted to gestational age-specific z-scores, multiples of the median or percentiles to allow comparison. Although this represents the most accurate way of indexing CO measurements in pregnancy, the availability of such constructed reference ranges is at present limited."[35] The current study provided reference interval graphs and tables (Supplements 4—6) and z-score equations for selected variables from Tables 1 and 2, and Supplement 2. In

TABLE 4
Pulsed Doppler vs continuous wave Doppler measurements

Measurement	Pulsed wave Doppler Mean (SD)	Continuous wave Doppler Mean (SD)	*P* value
Velocity time integral (cm)	21 (5)	23. (5)	.001
Heart rate/min	82 (14)	81.9 (14)	.85
Preload			
Stroke volume (mL)	66 (20)	72 (23)	.001
Stroke volume index (SV/BSA)	37 (14)	40 (15)	.003
Stroke work index (SV/MAP)	42 (21)	47 (23)	.005
Afterload			
Systemic vascular resistance (dynes×s/cm^5)	1420 (489)	1307 (580)	.003
Potential-to-kinetic energy ratio	38 (16)	35 (14)	.02
Contractility			
Inotropy (watts)	2.63 (1.17)	2.71 (1.38)	.37
Smith–Madigan inotropy index (watts/m^2)	1.46 (0.71)	1.5 (0.81)	.47
Blood flow			
Cardiac output (mL/min)	5.27 (1.68)	5.79 (1.87)	.001
Cardiac output index (CO/BSA)	2.93 (1.15)	3.23 (1.27)	.001

BSA, body surface area; *CO*, cardiac output; *MAP*, mean arterial pressure; *SD*, standard deviation; *SV*, stroke volume.
DeVore. Measurements of maternal cardiac function. Am J Obstet Gynecol 2023.

contrast, only 1 study by Vinayagam et al[40] in 2018 provided graphical reference ranges for the ascending aorta measurements of CO, SV, and systemic vascular resistance and a supplemental calculator to compute the centile for these measurements.

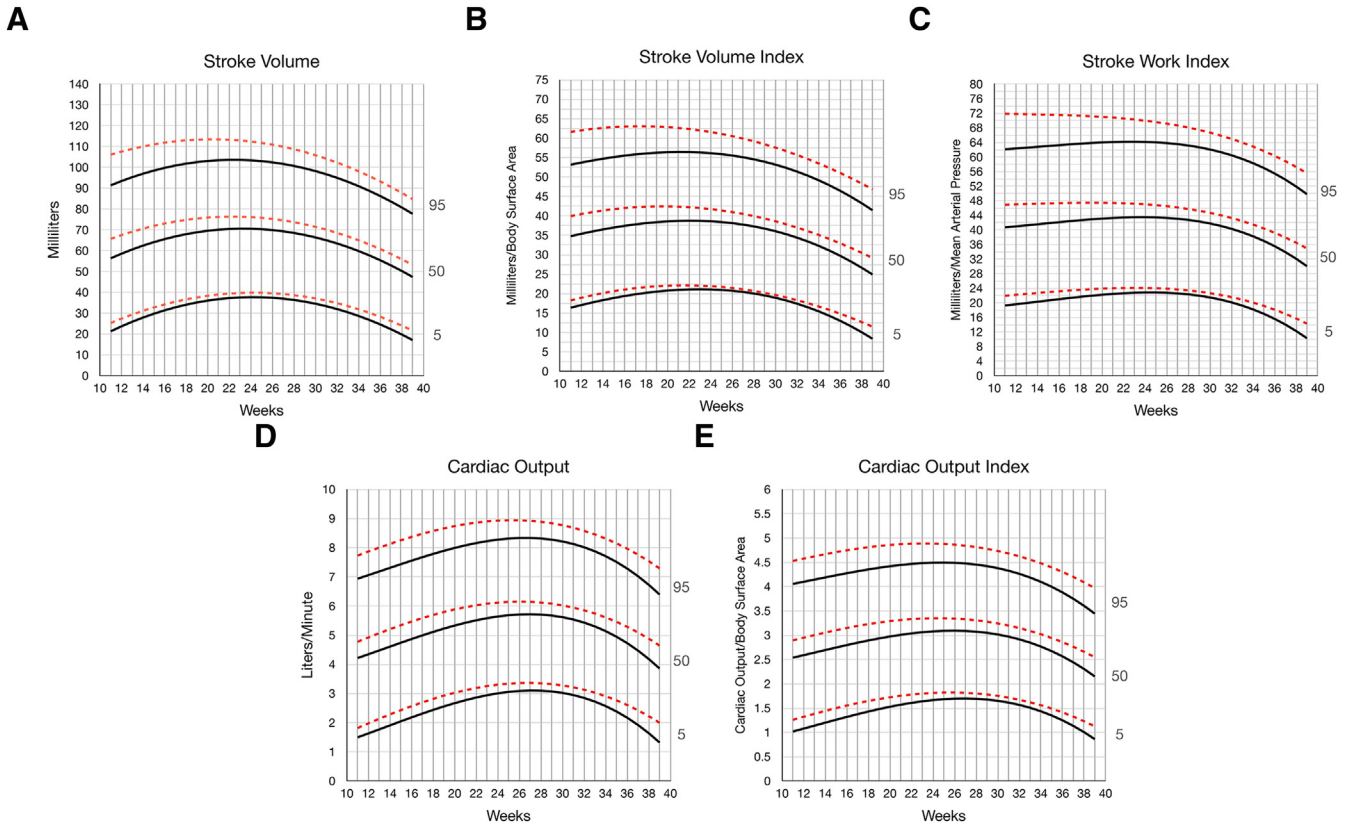
Results in the context of what is known

Given the findings listed in Table 5, and reviewed by Masini et al[19] in 2022, this study was undertaken to evaluate maternal cardiovascular function using an adult cardiac probe placed in the suprasternal notch. This had the advantages of recording a 2-dimensional image of the aortic arch from which the aortic diameter could be measured, and accurate placement of the PW Doppler sample volume and the CW Doppler line to record the VTI. The cardiac probe was used because it is available on almost all ultrasound machines used by physicians performing fetal ultrasound at a cost of only several thousand dollars. Given the above benefits of visualization of the aortic arch, accurate placement of the Doppler sample volume and CW recording line, the limitations of the USCOM device of deriving the aortic diameter from maternal height and obtaining the optimal continuous Doppler waveform by its characteristics and sound are negated.

All previous ultrasound studies in which SV and CO have been measured used the Doppler acquisition of the VTI from the ascending rather than the descending aorta (Table 5). When this study was initiated, we hoped that we could evaluate both the ascending and descending aorta, thus providing another imaging window to obtain measurements that would be compatible with previous studies using echocardiography or the USCOM, a CW device (Table 5). However, we found that imaging of the ascending aorta was possible in only a small percentage of patients. Therefore, this approach was not used as a screening tool because of the small sample size.

As shown in Figure 8, we compared the reference intervals for SV and CO from the current study and those from the study by Vinayagam et al[50] and found that SV and CO were lower at the level of the descending aorta than that of the ascending aorta. This would be expected because blood flow has been distributed to the head and upper extremities before sampling at the level distal to the left subclavian artery as it branches from the aorta. Because Vinayagam et al[50] did not provide tables of the mean and 5th and 95th reference intervals, we demonstrated in Figure 8 (at the 24-week point)

FIGURE 6
Reference interval graphs for stroke volume and cardiac output



Reference interval graphs of **A,** maternal stroke volume, **B,** stroke volume index, **C,** stroke work index, **D,** cardiac output, and **E,** cardiac output index. The (*red dotted lines*) represent measurements from the continuous wave Doppler and the (*black lines*) represent the pulsed Doppler results.

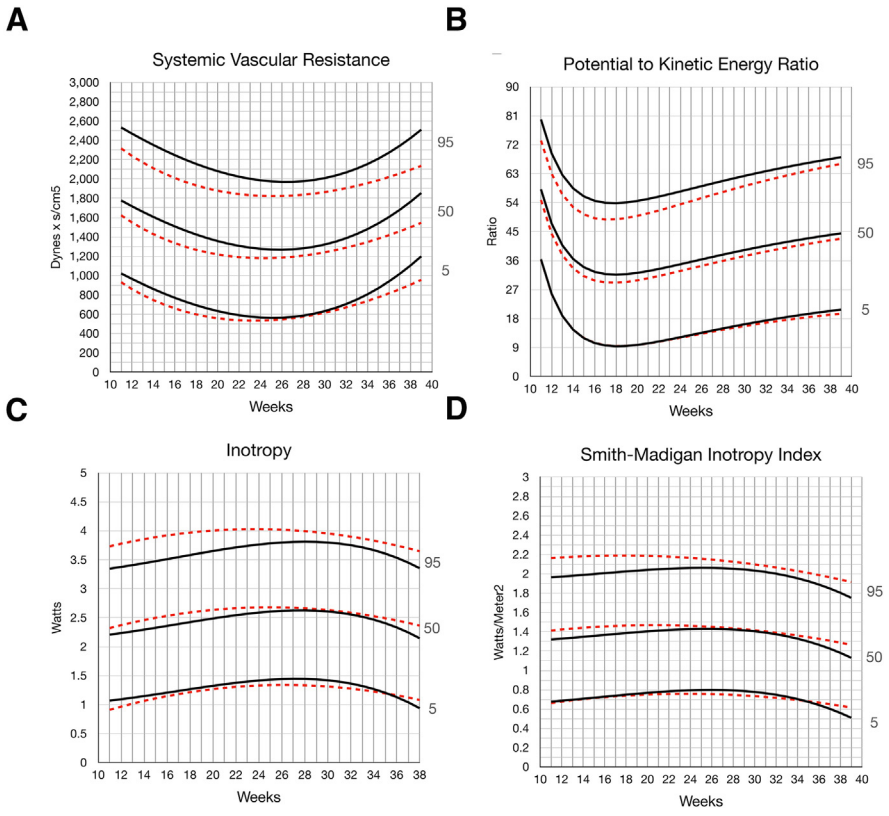
DeVore. Measurements of maternal cardiac function. Am J Obstet Gynecol 2023.

that the mean value for the SV was 85 mL in the Vinayagam et al study and 65 mL in this study, and that CO was 7 L/min and 4.8 L/min, respectively. This would suggest that 28% of the blood exiting the left ventricle was distributed to the head and upper extremities before being sampled in the descending aorta, which is in the range reported for blood flow distribution to the brain.[40,53]

Clinical implications

In 2019, the International Working Group on Maternal Hemodynamics reported different methods to measure CO that included 2 invasive methods using a pulmonary artery catheter, 7 minimally invasive methods, and 5 noninvasive methods.[3] Given the number of options for measuring CO, there are variations in "normal" values, depending on the method used.[3] Of the noninvasive methods, the 2 most commonly reported in the literature both involve transthoracic echocardiography, in which CO is computed either from measurements of the aortic diameter and VTI, or from the left ventricular end-diastolic and end-systolic images, from which the corresponding ventricular volumes are computed using the Simpson method (Figure 1). However, for screening purposes, a complete transthoracic echocardiogram is time-consuming, requires special training, and cannot be practically applied as a screening tool in conventional obstetrical practice. The second ultrasound tool that has been widely reported in the literature is the USCOM CW Doppler device that is blindly directed to the ascending aorta after placing the Doppler probe in the suprasternal notch.[40] The limitation of this approach is that the diameter of the aorta is derived from maternal height and not measured directly.[40] Because of the cost of the USCOM machine ($32,000) and the lack of other imaging modalities (2-D ultrasound, PW Doppler ultrasound, color Doppler ultrasound, and M-mode ultrasound), the device is not multifunctional. However, investigators who have used this device (Table 5) have

FIGURE 7
Reference interval graphs for afterload and contractility



Reference interval graphs of **A,** maternal systemic vascular resistance, **B,** potential-to-kinetic energy ratio, **C,** inotropy, and **D,** the Smith—Madigan inotropy index. The (*red dotted lines*) represent measurements from the continuous wave Doppler and the (*black lines*) represent the pulsed Doppler results.

DeVore. Measurements of maternal cardiac function. Am J Obstet Gynecol 2023.

provided important studies demonstrating the value of cardiovascular measurements listed in Tables 2 and 3 and Supplement 2.

This study provided additional measurements other than SV, CO, and systemic vascular resistance, as listed in Tables 2 and 3 and Supplement 2. Although almost all of the measurements listed in Table 2 are familiar to most investigators, the measurement of ventricular contractility or inotropy and the potential-to-kinetic energy ratio needs further explanation. In 2013, Smith and Madigan[44] proposed a noninvasive method to measure inotropy and preload (potential-to-kinetic energy ratio). Supplement 2 lists the measurements required for these 2 computations. All but one of the measurements can be obtained from the mean arterial pressure, VTI, heart rate, SV, and the mean pressure gradient, with the latter 4 available on the output of contemporary ultrasound machines. If the mean pressure gradient is not available, it can be computed using an equation that requires the peak velocity, VTI, and ejection time (Supplement 3).[54] The one measurement that is required to measure the potential-to-kinetic energy ratio is the maternal hemoglobin. We defaulted to a mean hemoglobin of 110 g/L because we found that adjusting the hemoglobin from 50 g/L to 180 g/L only changed the potential-to-kinetic ratio by <1.2%. Therefore, we recommend using the default hemoglobin value of 110 g/L, which is the average for pregnancy.[55,56]

The results of this study were divided into 4 groups: preload, afterload, contractility, and blood flow. Using this profile, the clinician may be able to provide useful clinical information by, for example, suggesting the optimal antihypertensive medication, such as labetalol if the hypertension is secondary to increased inotropy or CO.[19] Conversely, if the hypertension is secondary to increased systemic vascular resistance with a normal or low CO, drugs such as nifedipine or nitric oxide donors could be considered to lower peripheral resistance.[19,57]

Because the USCOM device used CW Doppler to measure the VTI, we used both PW and CW Doppler and found that the CW was significantly greater than the PW for all values except for the 2 contractillity measurements. This was most likely the result of the CW sampling of blood flow within the Doppler line, whereas the PW sampled a small segment of the blood flow. By providing results for both types of Doppler insonation, clinicians have a choice of either method when considering the clinical or research application of this methodology.

Research implications

To facilitate interpretation of the cardiovascular measurements for research purposes, we grouped them as follows: preload, afterload, contractility, and blood flow. Separating the cardiac measurements conceptually allows the examiner to clearly identify the mechanism of an abnormal measurement. To normalize measurements, as recommended by the International Working Group on Maternal Hemodynamics,[35] the preload measurement of SV was divided by the body surface area (SV index) and the mean arterial pressure (stroke work index). The afterload

TABLE 5
Previous studies using the Ultrasonic Cardiac Output Monitor (USCOM)

Study	Number of patients	Gestational age	Findings
Nonpregnant vs pregnant			
Khalil et al,[2] 2012	49 nonpregnant vs 185 pregnant	11–13 wk	Pregnant: ↑SV, CO, CI; ↓SVR, SVRI
Hypertension			
Verlohren et al,[11] 2017	129 HDP	Third trimester	↓ Cardiac output index ↑ Total vascular resistance
Preeclampsia			
Gagliardi et al,[12] 2017	12 preeclampsia	First trimester	↓ Cardiac output ↓ Inotropy index ↑ Total vascular resistance
Perry et al,[24] 2021	114 high BP and SGA fetuses, 202 high BP	26- to 41-wk gestation	↓ Cardiac output ↑ Total vascular resistance
Giannubilo et al,[52] 2017	48 preeclampsia	Third trimester	↓ Cardiac output ↑ Total vascular resistance
Abnormal fetal growth			
Farsetti et al,[14] 2022	36 SGA, 8 early FGR (<32 wk), 24 late FGR	Third trimester	↓ Cardiac output (early FGR vs SGA) ↑ Total vascular resistance (early FGR vs SGA)
Fetal distress in labor			
Mappa et al,[15] 2022	133 low-risk women (34 adverse outcome)	Third trimester	↑ Systemic vascular resistance ↑ Systemic vascular resistance index
Valensise et al,[16] 2018	77 patients (11; 14.3% had adverse outcome)	Third trimester	↓ Cardiac output ≤5.8 L/min ↓ Cardiac index ≤2.9 L/min/m^2 ↑ Total vascular resistance >1069 dynes×s/cm^5
Morbid obesity			
Vinayagam et al,[17] 2017	23 patients (BMI ≥40 kg/m^2)	Third trimester	↑MAP, HR, SVR ↓SVI and CI
Preterm PROM			
Valensise et al,[18] 2022	15 patients with pPROM	Third trimester	↑HR, CO ↓SVR
Preterm delivery			
Valensise et al,[25] 2016	48 SVR >1000 dynes×s/cm^5	Third trimester	↓ CO, COI, SV, SVI, SW, Inotropy I

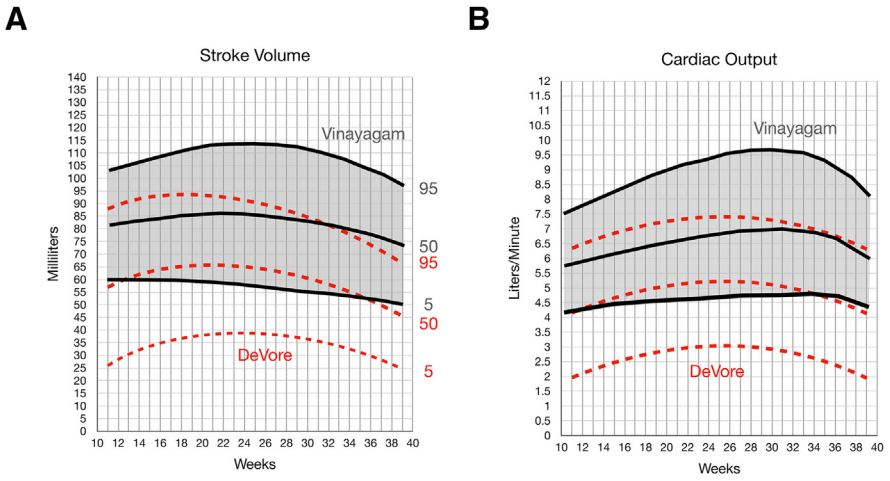
BMI, body mass index; *BP*, blood pressure; *CI*, cardiac index; *CO*, cardiac output; *COI*, cardiac output index; *FGR*, fetal growth restriction; *HDP*, hypertensive disease of pregnancy; *HR*, heart rate; *MAP*, mean arterial pressure; *pPROM*, preterm premature rupture of the membranes; *PROM*, premature rupture of the membranes; *SGA*, small for gestational age; *SV*, stroke volume; *SVI*, stroke volume index; *SVR*, systemic vascular resistance; *SVRI*, systemic vascular resistance index; *SW*, stroke work.

DeVore. Measurements of maternal cardiac function. Am J Obstet Gynecol 2023.

measurement of systemic vascular resistance was divided by the CO index (systemic vasculature resistance index). The contractility measurement was normalized by dividing the inotropy measurement by the body surface area (Smith–Madigan inotropy index). The blood flow measurement of CO was normalized by dividing it by the body surface area (CO index).

Although we have measured and computed several variables (Tables 1 and 2; Supplement 2), they are only useful if the required measurements and computations can be displayed in tabular or graphical formats such as the 5th, 50th, and 95th centiles, and results be displayed as a z-score and its corresponding centile so the examiner can use the information clinically or for research purposes. Supplements 4 to 6 are Excel spreadsheets that list the values for tables representing the 5th, 50th, and 95th centiles for the

FIGURE 8
Comparing descending and ascending aorta cardiac measurements



Using the aortic diameter computed from maternal height (cm), the **A,** stroke volume and **B,** cardiac output were compared between this study (*red lines*) and the study by Vinayagam et al[40] (*black lines* and *shaded area*).

DeVore. Measurements of maternal cardiac function. Am J Obstet Gynecol 2023.

measurements listed in Tables 1 and 2 and Supplement 2 that contain the mean, SD, and z-score equations. Figure 9 is a sample of the Excel calculator provided as Supplement 7 in which the examiner can select either the PW or CW option, using either pounds and inches or kilograms and centimeters. Acquiring the ultrasound image and making the measurements of the aortic diameter and VTI takes <2 minutes. Once the measurements are obtained, entry of data into the calculator takes <1 minute. From this profile, the examiner can determine if abnormal cardiac preload, afterload, contractility, or blood flow is present. In addition, we have found that the training required to be able to identify the descending aorta and acquire the VTI takes no more than 10 examinations before the examiner can be proficient (Supplement 1).

Finally, to test whether the measurements reported in this study are clinically useful, Table 6 lists results from 15 patients referred for fetal ultrasound because of maternal hypertension. The results are reported in centiles derived from their respective z-score values. The results demonstrated an incidence of >33% for increased mean arterial pressure, increased preload, afterload, contractility, and blood flow. However, unlike Verlohren et al,[11] who reported decreased CO, we found that only 13% of the 15 patients in our sample had decreased CO. Table 7 lists results from 8 patients with fetal growth restriction. Only 1 patient had an increased mean arterial pressure. The preload was <10th centile in 38%, the afterload was increased in over 50%, and blood flow was reduced in 50% of patients. These results are similar to those reported by Farsetti et al[14] in 2021. By sampling these 2 groups of patients, we were able to demonstrate the validity of our control z-score equations. However, larger clinical studies in high-risk patients, listed in Table 5, are required to further evaluate the results of our study.

Strengths and limitations

This study had the following strengths:

1. Using a cardiac probe that is available on almost all ultrasound machines used for fetal imaging.
2. Using a technique for imaging the descending aorta from the suprasternal notch, which provides direct visualization of the aorta to measure its diameter and placement of the PW sample volume and CW Doppler.
3. Grouping the results in 4 categories: preload, afterload, contractility, and blood flow, for easier clinical interpretation of the results.
4. Providing both tables and graphical displays of reference intervals for the 5th, 50th, and 95th centiles for measurements regressed against gestational age.
5. Providing an Excel calculator to compute the z-score and corresponding centile for several demographic measurements (weight, height, systolic blood pressure, diastolic blood pressure, and mean arterial pressure) and measurements of preload, afterload, contractility, and blood flow.
6. The technique described in this study would allow screening of high-risk patients in the obstetrical clinical milieu once a cardiac probe is acquired for their ultrasound machine used for fetal evaluation (Supplement 1).

A limitation of this study was that there is no other diagnostic tool that has been reported to compare measurements of the aortic diameter and VTI described in this study with the ascending aorta. However, a future study could be done to compare these measurements using the USCOM ultrasound device that can be placed in both the ascending and descending aorta.

Conclusions

Supplement 8 includes a video presentation summarizing the current study. The technique for evaluation of maternal cardiac function described in this study would allow screening of maternal left ventricular preload, afterload, contractility, and blood flow for either direct clinical application or further research. In addition, understanding the

FIGURE 9

Calculator for computing the z-score and corresponding centile for measurements of preload, afterload, contractility, and blood flow

Last	XXXX
First	YYYY
iD	123445
Age	34
Date	11/29/22
Maternal History	

Enter Data in Yellow Cells

Gestational Age

Weeks	34
Days	3

Maternal Height, Weight, Blood Pressure		Z-Score	Centile
Maternal Weight (Pounds)	180	0.21	58.35%
Maternal Height (Inches)	62	-0.39	34.71%
Systolic Bood Pressure (mmHg)	140	1.89	97.09%
Diastolic Blood Pressure (mm/Hg)	85	1.48	93.08%

Enter Measurements From Ultrasound Screen		Z-Score	Centile
Aortic Diameter (Centimeters)	2.00	0.09	53.76%
Heart Rate /Mininute	80	-0.51	30.51%
Mean Pressure Gradient (mmHG) (MnPG)	1.47		
Ejection Time (Milliseconds)	436		
Velocity Time Integral (VTI) (meters)	0.24		

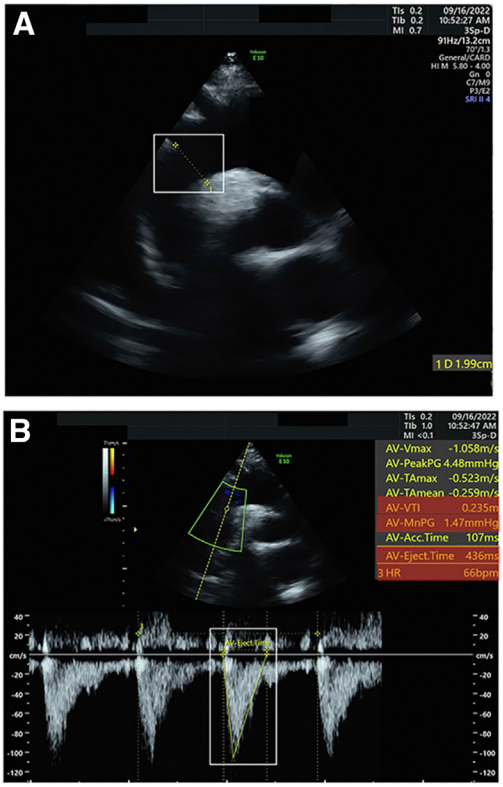
Computations		Z-Score	Centile
Weight (Kilograms)	81.65	0.21	58.35%
Height (Centimeters)	157.48	-0.39	34.71%
Body Surface Area (Meter^2)	1.89	0.13	55.16%
Mean Arterial Pressure (mmHg)	103.33	1.23	89.06%
Velocity Time Integral (Centimeter)	23.50	1.03	84.79%
Gestational Age (Weeks)	34.43		

Preload		Z-Score	Centile
Stroke Volume (milliliters)	73.79	0.79	78.40%
Stroke Volume Index (Stroke Volume/Body Surface Area)	39.05	0.71	76.14%
Stroke Work Index (Stroke Volume/Mean Arterial Pressure)	54.87	1.41	92.08%

Afterload		Z-Score	Centile
Systemic Vascular Resistance (Mean Arterial Presssure/Cardiac Output)	1400.37	-0.26	39.75%
Potential to Kinetic Energy Ratio	71	2.04	97.96%

Contractility		Z-Score	Centile
Inotropy (Watts)	2.36	-0.11	45.67%
Smith-Madigan Inotropy Index (Watts/Meter2)	1.25	-0.17	43.15%

Cardiac Blood Flow		Z-Score	Centile
Cardiac Output (Liters/Minute)	5.90	0.54	70.51%
Cardiac Output Index (Cardiac Output/Body Surface Area)	3.12	0.49	68.77%



A, Measurement of the descending aortic diameter (1D), **B,** Measurement of the velocity time integral (AV-VTI), heart rate (HR), mean pressure gradient (AV-MnPG), and ejection time (AV-Eject.Time).

AV-TAmax, aortic time average maximum velocity; *AV-TAmean*, aortic time average mean velocity; *AV-VTI*, aortic velocity time integral; *AV-MnPG*, aortic mean pressure gradient; *AV-Acc.Time*, aortic acceleration time; *AV-Eject.Time*, Aortic ejection time; *HR*, heart rate.

DeVore. Measurements of maternal cardiac function. Am J Obstet Gynecol 2023.

TABLE 6
Maternal history of hypertension: centiles computed from z-score values

				Preload			Afterload		Contractility		Blood flow	
Number	Gestational age, wk (d)	Other fetal findings	Mean arterial pressure	Stroke volume	Stroke volume index	Stroke work index	Systemic vascular resistance	Potential-to-kinetic energy ratio	Inotropy	SMII	Cardiac output	Cardiac output index
1	24 (3)		99.99%	99.96%	99.99%	99.99%	42.89%	99.99%	99.99%	99.99%	96.30%	99.57%
2	12 (6)		99.99%	39.06%	12.98%	44.70%	97.54%	99.71%	91.79%	55.02%	35.94%	14.28%
3	31 96)		65.09%	68.27%	72.73%	81.03%	30.05%	20.60%	66.51%	72.75%	71.37%	77.64%
4	23 (3)		89.95%	42.69%	41.38%	61.45%	44.59%	60.31%	66.48%	64.13%	64.94%	64.11%
5	23 (3)	FGR	97.14%	2.75%	2.12%	5.51%	99.93%	99.99%	10.98%	8.65%	5.37%	4.41%
6	35 (5)		96.04%	99.98%	99.99%	99.99%	5.88%	99.81%	100.00%	99.99%	99.80%	99.89%
7	13		99.99%	34.58%	16.98%	63.89%	88.48%	99.69%	97.67%	86.75%	57.99%	36.87%
8	13 (6)		98.33%	78.86%	71.93%	95.49%	53.85%	24.89%	92.04%	88.59%	69.38%	63.21%
9	12 (5)		99.99%	42.24%	40.86%	76.11%	85.13%	96.30%	82.60%	84.34%	42.70%	42.72%
10	24 (3)		99.99%	3.02%	4.71%	27.51%	99.99%	99.99%	7.88%	13.02%	1.19%	1.77%
11	38 (2)		96.40%	98.61%	96.78%	99.90%	14.92%	30.93%	99.86%	99.51%	94.63%	89.85%
12	35 (5)		96.04%	99.99%	99.99%	99.99%	5.88%	99.81%	99.99%	99.99%	99.80%	99.89%
13	24 (6)		94.81%	49.21%	24.29%	45.73%	82.75%	73.18%	53.28%	25.94%	28.16%	12.57%
14	28 (2)		36.07%	99.94%	99.88%	99.76%	9.34%	0.31%	100.00%	99.99%	98.30%	97.81%
15	32 (4)		86.07%	55.40%	55.76%	75.51%	39.06%	69.15%	51.44%	52.88%	70.11%	72.15%
<10th centile				2 (13%)	2 (13%)	1 (7%)	3 (20%)	1 (7%)	1 (7%)	1 (7%)	2 (13%)	2 (13%)
>90th centile			11 (73%)	5 (33%)	5 (33%)	6 (40%)	3 (20%)	8 (53%)	8 (53%)	5 (33%)	5 (33%)	4 (7%)

Red color indicate the values that are greater than the 90th percentile; green color indicate the values that are less than the 10th percentile.

FGR, fetal growth restriction; *SMII*, Smith—Madigan inotropy index.

DeVore. Measurements of maternal cardiac function. Am J Obstet Gynecol 2023.

TABLE 7
Patients with fetal growth restriction: centiles computed from z-score values

				Preload			Afterload		Contractility		Blood flow	
Number	Gestational age, wk (d)	Other fetal findings	Mean arterial pressure	Stroke volume	Stroke volume index	Stroke work index	Systemic vascular resistance	Potential-to-kinetic energy ratio	Inotropy	SMII	Cardiac output	Cardiac output index
1	19 (5)	Absent diastolic flow	**94.15%**	**5.79%**	**7.08%**	14.05%	**92.48%**	**99.84%**	26.36%	33.05%	17.83%	22.89%
2	32 (1)		58.60%	**1.24%**	**2.17%**	**2.70%**	**100.00%**	**99.40%**	**2.86%**	**5.83%**	**1.78%**	**3.27%**
3	33 (3)		34.74%	**7.71%**	10.35%	**9.66%**	**98.77%**	72.69%	**7.40%**	**9.87%**	**6.33%**	**8.11%**
4	22	Fetal TR	52.78%	45.35%	45.23%	47.52%	48.67%	34.62%	55.83%	53.96%	41.69%	41.24%
5	28 (4)	Dec RVF, bilateral PE	33.14%	**5.34%**	**6.20%**	**6.02%**	**97.35%**	**96.79%**	11.07%	13.44%	**5.14%**	**6.19%**
6	32 (4)	Dec CPR	26.34%	25.38%	20.00%	16.70%	**90.57%**	**96.79%**	**8.55%**	**6.24%**	**9.84%**	**7.19%**
7	37 (2)		20.73%	34.98%	44.38%	36.25%	64.24%	80.72%	23.75%	28.07%	28.45%	32.99%
8	37 (3)	Fetal PE	25.77%	30.28%	33.72%	28.89%	**99.38%**	67.07%	24.15%	23.56%	10.89%	**9.57%**
<10th centile				4 (50%)	3 (38%)	3 (38%)			3 (38%)	3 (38%)	4 (50%)	4 (50%)
>90th centile			1 (13%)				6 (75%)	4 (50%)				

Red color indicate the values that are greater than the 90th percentile; green color indicate the values that are less than the 10th percentile.

CPR, cerebroplacental ratio; *Dec*, decreased; *PE*, pericardial effusion; *RVF*, right ventricular function; *SMII*, Smith–Madigan inotropy index; *TR*, tricuspid regurgitation.

DeVore. Measurements of maternal cardiac function. Am J Obstet Gynecol 2023.

cardiovascular profile of the patient would allow the clinician to use the appropriate hypertensive drugs according to the results.

Acknowledgments

The authors would like to thank the following individuals who participated in acquiring clinical information and are employed by the Fetal Diagnostic Centers: Idella Houston; Angelica Hernandez; Rosio Anzora; Tejera Navarro; Deborah Baez; Nicole Sewell; April Ante-Sanchez; Guillermina Torres; Evelyn Crisp; and Cecilia Castorena. ■

References

1. Erez O, Romero R, Jung E, et al. Preeclampsia and eclampsia: the conceptual evolution of a syndrome. Am J Obstet Gynecol 2022;226:S786–803.

2. Khalil A, Goodyear G, Joseph E, Khalil A. PP097. Cardiac output and systemic vascular resistance in normal pregnancy and in control non-pregnant women. Pregnancy Hypertens 2012;2:292–3.

3. Cornette J, Roos-Hesselink JW. Normal cardiovascular adaptation to pregnancy. In: Stergiopoulos K, Brown DL, eds. Evidence-based cardiology consult. London: Springer London; 2014:423–432. https://link.springer.com/chapter/10.1007/978-1-4471-4441-0_29. Accessed February 3, 2023.

4. Kager CC, Dekker GA, Stam MC. Measurement of cardiac output in normal pregnancy by a non-invasive two-dimensional independent Doppler device. Aust N Z J Obstet Gynaecol 2009;49:142–4.

5. Lee W, Rokey R, Cotton DB. Noninvasive maternal stroke volume and cardiac output determinations by pulsed Doppler echocardiography. Am J Obstet Gynecol 1988;158:505–10.

6. Melchiorre K, Giorgione V, Thilaganathan B. The placenta and preeclampsia: villain or victim? Am J Obstet Gynecol 2022;226:S954–62.

7. Ferrazzi E, Stampalija T, Monasta L, Di Martino D, Vonck S, Gyselaers W. Maternal hemodynamics: a method to classify hypertensive disorders of pregnancy. Am J Obstet Gynecol 2018;218:124.e1–11.

8. Gyselaers W. Hemodynamic pathways of gestational hypertension and preeclampsia. Am J Obstet Gynecol 2022;226:S988–1005.

9. Tay J, Foo L, Masini G, et al. Early and late preeclampsia are characterized by high cardiac output, but in the presence of fetal growth restriction, cardiac output is low: insights from a prospective study. Am J Obstet Gynecol 2018;218:517.e1–12.

10. Tay J, Masini G, McEniery CM, et al. Uterine and fetal placental Doppler indices are associated with maternal cardiovascular function. Am J Obstet Gynecol 2019;220:96.e1–8.

11. Verlohren S, Perschel FH, Thilaganathan B, et al. Angiogenic markers and cardiovascular indices in the prediction of hypertensive disorders of pregnancy. Hypertension 2017;69:1192–7.

12. Gagliardi G, Tiralongo GM, LoPresti D, et al. Screening for pre-eclampsia in the first trimester: role of maternal hemodynamics and bioimpedance in non-obese patients. Ultrasound Obstet Gynecol 2017;50:584–8.

13. Perry H, Lehmann H, Mantovani E, Thilaganathan B, Khalil A. Are maternal hemodynamic indices markers of fetal growth restriction in pregnancies with a small-for-gestational-age fetus? Ultrasound Obstet Gynecol 2020;55:210–6.

14. Farsetti D, Pometti F, Tiralongo GM, et al. Distinction between SGA and FGR by means of fetal umbilical vein flow and maternal hemodynamics. J Matern Fetal Neonatal Med 2022;35:6593–9.

15. Mappa I, Luviso M, Tartaglia S, et al. Maternal cardiovascular function in the prediction of fetal distress in labor: a prospective cohort study. J Matern Fetal Neonatal Med 2022;35:7139–45.

16. Valensise H, Tiralongo GM, Pisani I, et al. Maternal hemodynamics early in labor: a possible link with obstetric risk? Ultrasound Obstet Gynecol 2018;51:509–13.

17. Vinayagam D, Gutierrez J, Binder J, Mantovani E, Thilaganathan B, Khalil A. Impaired maternal hemodynamics in morbidly obese women: a case-control study. Ultrasound Obstet Gynecol 2017;50:761–5.

18. Valensise H, Pometti F, Farsetti D, Novelli GP, Vasapollo B. Hemodynamic assessment in patients with preterm premature rupture of the membranes (pPROM). Eur J Obstet Gynecol Reprod Biol 2022;274:1–4.

19. Masini G, Foo LF, Tay J, et al. Preeclampsia has two phenotypes which require different treatment strategies. Am J Obstet Gynecol 2022;226:S1006–18.

20. Valensise H, Farsetti D, Pometti F, Vasapollo B, Novelli GP, Lees C. The cardiac-fetal-placental unit: fetal umbilical vein flow rate is linked to the maternal cardiac profile in fetal growth restriction. Am J Obstet Gynecol 2022 [Epub ahead of print].

21. Vasapollo B, Novelli GP, Gagliardi G, Farsetti D, Valensise H. Pregnancy complications in chronic hypertensive patients are linked to pre-pregnancy maternal cardiac function and structure. Am J Obstet Gynecol 2020;223:425.e1–13.

22. Dennehy N, Lees C. Preeclampsia: maternal cardiovascular function and optimising outcomes. Early Hum Dev 2022;174:105669.

23. Yagel S, Cohen SM, Goldman-Wohl D. An integrated model of preeclampsia: a multifaceted syndrome of the maternal cardiovascular-placental-fetal array. Am J Obstet Gynecol 2022;226:S963–72.

24. Perry H, Binder J, Gutierrez J, Thilaganathan B, Khalil A. Maternal haemodynamic function differs in pre-eclampsia when it is associated with a small-for-gestational-age newborn: a prospective cohort study. BJOG 2021;128:167–75.

25. Valensise H, Farsetti D, Lo Presti D, et al. Preterm delivery and elevated maternal total vascular resistance: signs of suboptimal cardiovascular adaptation to pregnancy? Ultrasound Obstet Gynecol 2016;48:491–5.

26. Valensise H, Lo Presti D, Tiralongo GM, et al. Foetal heart rate deceleration with combined spinal-epidural analgesia during labour: a maternal haemodynamic cardiac study. J Matern Fetal Neonatal Med 2016;29:1980–6.

27. Aderibigbe OA, Hackney DN, Ranzini AC, Lappen JR. Tight vs liberal control of mild postpartum hypertension: a randomized controlled trial. Am J Obstet Gynecol MFM 2022;5:100818.

28. Magee LA, Khalil A, Kametas N, von Dadelszen P. Toward personalized management of chronic hypertension in pregnancy. Am J Obstet Gynecol 2022;226:S1196–210.

29. Aliyu Z, Kushimo OA, Oluwole AA, et al. Effects of pregnancy on cardiac structure and function in women with sickle cell anemia: a longitudinal comparative study. J Matern Fetal Neonatal Med 2022;35:10049–54.

30. Chen Y, Chen Q, Wu Y, et al. Fetal cardiac geometry and function in pregnancies with well-controlled gestational diabetes mellitus using Fetal HQ. J Matern Fetal Neonatal Med 2022;35:8331–7.

31. DeVore GR, Afshar Y, Harake D, Satou G, Sklansky M. Speckle-tracking analysis in fetuses with tetralogy of Fallot: evaluation of right and left ventricular contractility and left ventricular function. J Ultrasound Med 2022;41:2955–64.

32. Oluklu D, Menekse Beser D, Uyan Hendem D, et al. Assessment of fetal cardiac morphology and functional changes in early-onset and late-onset fetal growth restriction. Int J Gynaecol Obstet 2022 [Epub ahead of print].

33. Huang P, Deng Y, Feng L, Gao Y, Cheng X, Liu H. Evaluation of fetal cardiac function in maternal gestational diabetes mellitus by speckle-tracking echocardiography. J Ultrasound Med 2023;42:81–9.

34. DeVore GR, Gumina DL, Hobbins JC. Assessment of ventricular contractility in fetuses with an estimated fetal weight less than the tenth centile. Am J Obstet Gynecol 2019;221:498.e1–22.

35. Bijl RC, Valensise H, Novelli GP, et al. Methods and considerations concerning cardiac output measurement in pregnant women: recommendations of the International Working Group on Maternal Hemodynamics. Ultrasound Obstet Gynecol 2019;54:35–50.

36. Mulder E, Basit S, Oben J, van Kuijk S, Ghossein-Doha C, Spaanderman M. Accuracy and precision of USCOM versus transthoracic echocardiography before and during pregnancy. Pregnancy Hypertens 2019;17:138–43.

37. Easterling TR, Watts DH, Schmucker BC, Benedetti TJ. Measurement of cardiac output during pregnancy: validation of Doppler

technique and clinical observations in pre-eclampsia. Obstet Gynecol 1987;69:845–50.
38. van Oppen AC, Stigter RH, Bruinse HW. Cardiac output in normal pregnancy: a critical review. Obstet Gynecol 1996;87:310–8.
39. Vinayagam D, Patey O, Thilaganathan B, Khalil A. Cardiac output assessment in pregnancy: comparison of two automated monitors with echocardiography. Ultrasound Obstet Gynecol 2017;49:32–8.
40. Vinayagam D, Thilaganathan B, Stirrup O, Mantovani E, Khalil A. Maternal hemodynamics in normal pregnancy: reference ranges and role of maternal characteristics. Ultrasound Obstet Gynecol 2018;51:665–71.
41. Montaguti E, Youssef A, Cavalera M, et al. Maternal hemodynamic assessment by USCOM® device in the first trimester of pregnancy. J Matern Fetal Neonatal Med 2022;35:5580–6.
42. Mangos JG, Pettit F, Preece R, Harris K, Brown MA. Repeatability of USCOM®-measured cardiac output in normotensive non-pregnant and pregnant women. Pregnancy Hypertens 2018;12:71–4.
43. Altman DG, Chitty LS. Design and analysis of studies to derive charts of fetal size. Ultrasound Obstet Gynecol 1993;3:378–84.
44. Smith BE, Madigan VM. Non-invasive method for rapid bedside estimation of inotropy: theory and preliminary clinical validation. Br J Anaesth 2013;111:580–8.
45. American Institute of Ultrasound in Medicine. AIUM-ACR-ACOG-SMFM-SRU practice parameter for the performance of standard diagnostic obstetric ultrasound examinations. J Ultrasound Med 2018;37:E13–24.
46. Salomon LJ, Alfirevic Z, Berghella V, et al. ISUOG Practice Guidelines (updated): performance of the routine mid-trimester fetal ultrasound scan. Ultrasound Obstet Gynecol 2022;59:840–56.
47. AIUM practice parameter for the performance of detailed second- and third-trimester diagnostic obstetric ultrasound examinations. J Ultrasound Med 2019;38:3093–100.
48. DeVore GR. Computing the Z score and centiles for cross-sectional analysis: a practical approach. J Ultrasound Med 2017;36:459–73.
49. Nidorf SM, Picard MH, Triulzi MO, et al. New perspectives in the assessment of cardiac chamber dimensions during development and adulthood. J Am Coll Cardiol 1992;19:983–8.
50. Vinayagam D, Bowe S, Sheehan E, Thilaganathan B, Khalil A. Non-invasive haemodynamic monitoring in pregnancy: a comparative study using ultrasound and bioreactance. Fetal Diagn Ther 2017;41:273–82.
51. Sanghavi M, Rutherford JD. Cardiovascular physiology of pregnancy. Circulation 2014;130:1003–8.
52. Giannubilo SR, Pasculli A, Tidu E, Biagini A, Boscarato V, Ciavattini A. Relationship between maternal hemodynamics and plasma natriuretic peptide concentrations during pregnancy complicated by preeclampsia and fetal growth restriction. J Perinatol 2017;37:484–7.
53. Xing CY, Tarumi T, Liu J, et al. Distribution of cardiac output to the brain across the adult lifespan. J Cereb Blood Flow Metab 2017;37:2848–56.
54. Zhang Y, Nitter-Hauge S. Determination of the mean pressure gradient in aortic stenosis by Doppler echocardiography. Eur Heart J 1985;6:999–1005.
55. Khoigani MG, Goli S, Hasanzadeh A. The relationship of hemoglobin and hematocrit in the first and second half of pregnancy with pregnancy outcome. Iran J Nurs Midwifery Res 2012;17:S165–70.
56. Shinar S, Shapira U, Maslovitz S. Redefining normal hemoglobin and anemia in singleton and twin pregnancies. Int J Gynaecol Obstet 2018;142:42–7.
57. Lees C, Valensise H, Black R, et al. The efficacy and fetal-maternal cardiovascular effects of transdermal Glyceryl trinitrate in the prophylaxis of pre-eclampsia and its complications: a randomized double-blind placebo-controlled trial. Ultrasound Obstet Gynecol 1998;12:334–8.

Author and article information

From the Fetal Diagnostic Centers, Pasadena and Lancaster, CA (Drs DeVore and Polanco); Department of Obstetrics and Gynecology, University of California, Los Angeles School of Medicine, Los Angeles, CA (Dr DeVore); and Department of Obstetrics and Gynecology, Wayne State University, Detroit, MI (Dr DeVore).

Received Nov. 30, 2022; revised Dec. 30, 2022; accepted Jan. 3, 2023.

The authors report no conflict of interest.

This study did not receive any financial support.

Corresponding author: Greggory R. DeVore, MD. grdevore@gmail.com